archaeometry

Archaeometry **54**, 2 (2012) 278–293 doi: 10.1111/j.1475-4754.2011.00617.x

PIGMENTS AND PLASTERS FROM THE ROMAN SETTLEMENT OF *THAMUSIDA* (RABAT, MOROCCO)*

E. GLIOZZO,[1]† F. CAVARI,[2] D. DAMIANI[1] and I. MEMMI[1]

[1]*Dipartimento di Scienze della Terra, Università di Siena, via Laterina 8, 53100 Siena, Italy*
[2]*Dipartimento di Archeologia e Storia delle Arti, Università di Siena, via Roma 56, 53100 Siena, Italy*

A total of 22 samples were taken both from plasters still in situ *and from collapsed material recovered by French, Italian and Moroccan teams at the Roman settlement of* Thamusida *(Rabat, Morocco). The sample characterization was obtained using optical microscopy, scanning electron microscopy, image analysis and Raman micro-spectroscopy. Plaster aggregate was made using a mixture of sands and clays that outcrop nearby, while lime was probably produced using the local limestone crust, as was further verified for the mortars. The plasters from the bath complexes (public buildings) and the* Temple à trois cellae *(sacred building) were very poorly made, while those from areas VII and XX (private buildings) indicated the involvement of more expert masons. The pigments used were cinnabar, red ochre, yellow ochre, Egyptian blue, green earth, chalk white and carbon black. The overall manufacture was of low quality, and hence perfectly comparable to that observed in other Roman Provinces. With respect to Italy and to other Mediterranean Roman sites,* Thamusida *fits well within an aesthetic and technical* koinè *that differentiates sites of the Italian peninsula from those in the Provinces.*

KEYWORDS: PLASTERS, PIGMENTS, THAMUSIDA, MOROCCO

INTRODUCTION

In the first century AD, *Thamusida* was founded by the Romans on a plateau immediately to the south of the Oued Sebou floodplain, about 45 km north of Rabat (Callu *et al*. 1965; Hallier *et al*. 1970; Marion and Rebuffat 1977). Archaeological excavation brought to light numerous classes of material that underwent archaeometric investigation (e.g., stone materials, mortars, ceramics and glasses; Gliozzo *et al*. 2009a–c, 2010, 2011a,b). This paper concerns both the plasters and the pigments found by the French, Italian and Moroccan teams who carried out the study of the settlement. The characterization of the plasters, together with the study of building techniques, decisively contributes to the historical and archaeological reconstruction (Barbet 1998). At *Thamusida*, the discovery of painted plasters in public, sacred and private buildings indicates their widespread and diachronic use through the different periods of Roman life (see Cavari 2008). As for pigments, their composition and origin are discussed by ancient writers as well as by modern archaeologists and archaeometrists (e.g., Delamare 1983; Damiani *et al*. 2003; Pagès-Camagna and Colinart 2003; Baraldi *et al*. 2006; Edwards *et al*. 2009, Duran *et al*. 2010; Hradil *et al*. 2010; Mazzocchin *et al*. 2010). Vitruvius, Pliny and *Theophrastos* (but also *Celsus* or *Dioscorides* and others) provided valuable information regarding both issues. Unfortunately, this information does not always agree, possibly being inaccurate or difficult to interpret (see, e.g., Reinach 1985; Béarat 1997; Gliozzo 2007). The reconstruction of trade routes is complicated by the wide availability of many raw materials, by inexorable post-depositional processes and by restrictions associated with

*Received 4 October 2010; accepted 22 March 2011
†Corresponding author: email gliozzo@unisi.it

the analytical methods. Archaeometric research on Moroccan pigments has not been performed so far, thus conferring originality and novelty to this study.

The research seeks to determine: (1) the chemical and mineralogical composition of the plasters; (2) the reconstruction of the production technology (i.e., quantification and characterization of layers applied, presence/absence of additives, quality of the execution); (3) the pigment identification; and (4) the chemical and mineralogical composition of two beads of blue pigment found on the site.

MATERIALS

In order to obtain a representative repertory in term of macroscopic characteristics, chronology and site distribution, the samples analysed here were selected from plasters still conserved *in situ* and from among fragmented materials recovered by French and Italian–Moroccan archaeological teams (Fig. 1 (a)). A total of 22 samples (Table 1) were collected: 13 samples from the *Thermes du fleuve* (building V.1.1), four samples from area VII, one sample from the *Temple à trois cellae* (building IV.1.1), two samples from area XX and two samples from area XXXVII.

Samples

Thermes du fleuve *(building V.1.1)* Samples THi 1–4 were found by the French team and kept in a box labelled as '*Thermes du fleuve'*. The fragments formed a part of a unitary geometric design, showing red bands on a white ground, alternating with green or yellow fields. All of them are further characterized by a rough and streaked surface. Taken from plasters still *in situ*, samples THi 5–13 show red bands on a white ground (THi 5–8), a yellow and red decoration that may be imitating marble (THi 10) or a single colour (green in THi 9 and 13, black in THi 11, red in THi 12). Samples THi 9 and 13 are characterized by abundant inclusions, possibly including crushed ceramics (chamotte; for the use of this term, see Cuomo di Caprio and Vaughan 1993).

Area VII This area was excavated in 2003 in the northeastern part of the settlement. Samples THi 14 and THi 16–18 are part of a consistent set of decorated fragments, showing red and dark blue fields (Fig. 1 (b)). These plasters are characterized by a high concentration of coarse grains, resulting in a pinkish colour.

Temple à trois cellae *(building IV.1.1)* The poorly preserved undecorated plasters did not allow extensive sampling (THi 15). However, it would be interesting to verify whether the prestige of the building led to a technical improvement.

Area XX The area was excavated from 2003 to 2004 in the northeastern part of the settlement. Sample THi 19 (Fig. 1 (c)) shows yellow and black fields divided by a white strip, while THi 20 displays yellow and blue fields divided by a red strip. Both samples are characterized by a smooth paint layer, typical of first century AD paintings. They should be related to an earlier building, whose materials were reused for filling a levelling layer; the latter served for the construction of a new building in the second half of the second century AD.

Area XXXVII Samples THi 22 and 23 are two beads of blue pigment (Ø 1.5–2.0 cm; Fig. 1 (d)). A few other examples were stored in the *Thamusida* warehouses, but no indication of their origin

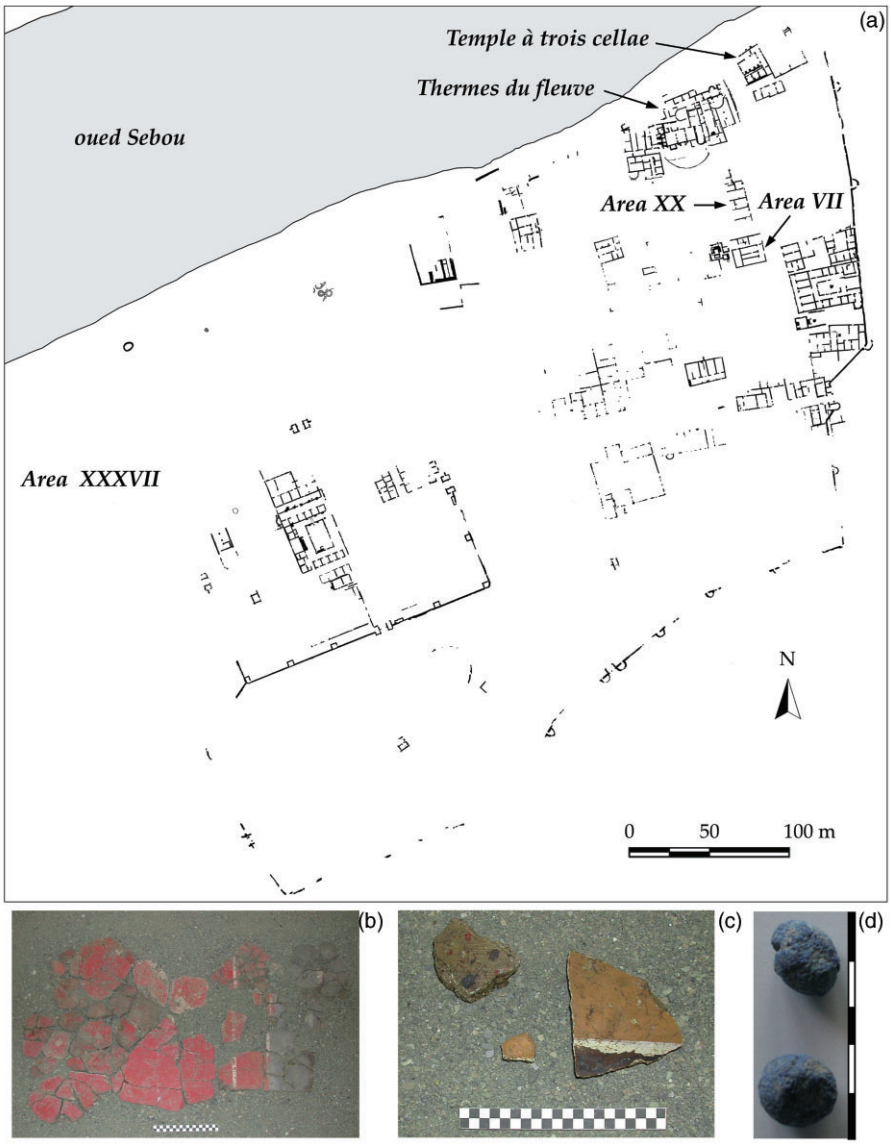

Figure 1 *(a) A map of the* Thamusida *settlement. (b) Fragments recovered from area VII. (c) Sporadic fragments from area XX. (d) Two beads of blue pigment (see online for a colour version of this figure).*

has been preserved. At the macroscopic scale, the beads show blue microcrystals, associated with minute transparent crystals. A yellow encrustation unevenly covers the surface.

EXPERIMENTAL

Thin sections were obtained for all samples. The plaster was cut perpendicular to the painted surface, in order to obtain the profile of the stratigraphic sequence. The thin sections were

Table 1 *The sample list*

Sample	*Pigment*	*Building, area, room*	*Positioning*	*Chronology (AD)*
THi 1	Dark red + white	V.1.1 (*Thermes du fleuve*)?	–	Second to third century
THi 2	Dark red	V.1.1 (*Thermes du fleuve*)?	–	Second to third century
THi 3	Dark red	V.1.1 (*Thermes du fleuve*)?	–	Second to third century
THi 4	Dark yellow	V.1.1 (*Thermes du fleuve*)?	–	Second to third century
THi 5	White	V.1.1 (*Thermes du fleuve*), room 25	162	End of second to beginning/first half of third century
THi 6	White	V.1.1 (*Thermes du fleuve*), room 25	152	End of second to beginning/first half of third century
THi 7	White	V.1.1 (*Thermes du fleuve*), room 25	150	End of second to beginning/first half of third century
THi 8	White	V.1.1 (*Thermes du fleuve*), room 25	150	End of second to beginning/first half of third century
THi 9	Green	V.1.1 (*Thermes du fleuve*), room 25	161	End of second to beginning/first half of third century
THi 10	Dark red	V.1.1 (*Thermes du fleuve*), room 36	228	End of second to beginning/first half of third century
THi 11	Dark green	V.1.1 (*Thermes du fleuve*), room 24	30	Third century, earlier than THi 12
THi 12	Dark red + white	V.1.1 (*Thermes du fleuve*), room 24	398	Third century, later than THi 12
THi 13	Green	V.1.1 (*Thermes du fleuve*), room 25	161	End of second to beginning/first half of third century
THi 14	Bright red	Area VII, room 2	7073	Second half of first century
THi 15	White	IV.1.1 (*Temple à trois cellae*)	Back wall, west cell	Second half of first century
THi 16	Bright red	Area VII, room 2	7073	Second half of first century
THi 17	Bright red	Area VII, room 2	7073	Second half of first century
THi 18	Dark blue	Area VII, room 2	7073	Second half of first century
THi 19	Light yellow + black	Area XX, building 2	20119	End of first half of first century
THi 20	Blue, dark red, dark yellow	Area XX, building 2	20028	End of first half of first century
THi 22	Blue	Area XXXVII	37012	–
THi 23	Blue	Area XXXVII	37018	–

observed by optical microscopy and scanning electron microscopy. Optical microscopy was used to identify the mineralogical phases. Scanning electron microscopy (SEM–EDS) was employed for a detailed description of the plaster layers, both in terms of textural features and chemical composition. The chemical analyses were performed for both crystals (aggregate) and matrices (binders). EDS analysis on large areas (at least 20 μm on each side) was used to obtain representative average values of the matrix composition. Matrix (including both binder and fine fraction of sand <63 μm), skeleton (coarser aggregate > matrix), percentage porosity and average grain-size were determined by image analysis, applying the method provided by Carò and Di Giulio (2004). Each sample was photographed in detail, in order to reconstruct an area of 2 cm^2; the resulting collage of images was subjected to image analysis using Image Pro Plus software.

The scanning electron microscope used was a Philips XL30, equipped with an energy-dispersive spectrometer (EDS) Philips EDAX DX4. A variety of natural and synthetic materials were used as primary and quality control standards. Operating conditions were as follows: accelerating voltage 20 kV, beam current ~30–40 mA and a working distance of 10–15 mm. To control the accuracy of the results, the EDX quantitative microanalyses with the theoretical inner pattern were obtained by using the ZAF method of correction.

Pigment characterization was obtained directly on the samples by Raman micro-spectroscopy, without any prior preparation. Instrumentation consisted of a Jobin Ivon Ltd integrated LABRAM confocal spectrometer equipped with a CCD detector, an Ar^+ laser ($\lambda = 514.5$ nm) and Notch holographic filters. The spectral resolution was 1.5 cm^{-1}. The two beads of blue pigment were characterized by both Raman micro-spectroscopy and scanning electron microscopy.

RESULTS

Plasters

The *Thamusida* plasters show three superimposed layers below the pigment. The first layer is the one applied to the wall and the third layer represents the thin ground for the application of the pigment, while the second layer is intermediate between the first and the second. Two exceptions are represented by samples THi 5 (discussed below) and 15. The former shows three superimposed phases of three layers each; the latter consists of a single thick layer, without any internal distinction or surface finishing.

First layer The percentage of skeleton always exceeds that of the matrix (Table 2). The latter is composed mainly of CaO, with minor amounts of SiO_2 and Al_2O_3. The matrix composition (Table 2) is rather heterogeneous within a single sample, but a trend can be noticed when grouping samples by building. With respect to samples THi 1–4, samples THi 14 and 16–18 show the lowest CaO (average value) and the highest SiO_2 and Al_2O_3 contents. The mineralogical assemblage is made of quartz, calcite, feldspars, rare phyllosilicates, pyroxenes, garnets and amphiboles, numerous epidotes *s.s.* and other accessory minerals. The ubiquitous quartz shows angular to subrounded habitus, low sphericity and crystal dimensions not exceeding 500 μm. The abundant calcite shows variable dimensions (up to 1 mm) and is frequently highly fractured. Among feldspars, orthoclase and albite are frequent; crystals are generally sub-rounded, sometimes very fractured and zoned (usually K-feldspar in the core and albite to the edge, but also vice versa). The composition of K-feldspar is generally stoichiometric, but sanidine may contain small amounts of Ca. The composition of plagioclases is mostly albitic, but labradorite is present as well. Among phyllosilicates, biotite and small crystals of chlorites are prevalent. The former

Table 2 *First layer: the percentages of porosity, matrix and skeleton and the average grain-size obtained by image analysis. Matrix composition obtained by SEM–EDS (five areas of at least 20 μm side × each sample). THi 5 data refer to the first phase; image analysis was not performed*

	THi 1–4		*THi 5*		*THi 6–13*		*THi 14, 16–18*		*THi19–20*		*THi 15*	
Image analysis												
Porosity	18%		–		23%		21%		20%		18%	
Matrix	35%		–		33%		28%		25%		30%	
Skeleton	47%		–		44%		51%		55%		52%	
Grain average dimensions	250 μm		–		300 μm		300 μm		400 μm		300 μm	
SEM–EDS	*n = 20*	*s.d.*	*n = 5*	*s.d.*	*n = 45*	*s.d.*	*n = 20*	*s.d.*	*n = 10*	*s.d.*	*n = 5*	*s.d.*
SiO_2	6.6	0.8	12.1	5.1	14.8	6.2	14.5	3.2	14.5	0.9	13.8	4.9
TiO_2	0.2	0.2	0.3	0.2	0.2	0.1	0.3	0.2	0.4	0.6	0.2	0.2
Cr_2O_3	0.2	0.3	0	0	0.1	0.2	0.4	0.5	0.4	0.3	0.3	0.4
Al_2O_3	1.1	0.4	2.8	1.7	2.2	1.0	4.7	0.5	2.9	0.3	4.8	1.1
FeO	1.2	0.3	1.7	0.9	1.4	0.7	4.2	0.6	2.2	0.9	7.3	3.2
MnO	0.3	0.3	0.4	0.3	0.2	0.2	0.5	0.4	0.6	0.4	0.2	0.3
MgO	1.8	1.2	1.4	2.1	1.5	0.4	4.7	2.4	5.6	0.2	1.1	2.4
CaO	87.7	1.5	80.2	5.1	78.4	7.2	68.2	6.1	71.1	2.6	71.4	6.2
Na_2O	0.7	0.7	0.7	0.8	0.7	0.3	1.9	0.5	1.9	0.6	0.6	0.7
K_2O	0.1	0.2	0.4	0.4	0.6	0.7	0.9	0.5	0.7	0.4	0.3	0.4
Tot.	100		100		100		100		100		100	

frequently shows apatite and zircon inclusions and a weakly chloritized composition. The chlorites are Mg- and Fe-rich. Sporadic muscovite shows variable compositions, especially in relation to K_2O and FeO contents; in one case, it appears to derive from sillimanite alteration. The latter shows a stoichiometric composition, with minor impurities due to the presence of alkali, Ti, Mg, Mn and Cr. The rare pyroxenes show crystals of small dimensions (average of 50 μm), with augite (frequently sub-calcic) prevailing over orthopyroxenes. The rare garnets are generally colourless and microfractured, sometimes altered to chlorite. The compositions are intermediate between a pyrope and an Fe-rich almandine, or between an andradite and a grossular. Ortho- and clino-amphiboles are characterized by non-stoichiometric compositions, resembling that of gedrite or anthophyllite and that of pargasite or edenite, respectively. Rare anhedral crystals of Ca-silicates have been observed by SEM–EDS only; their composition resembles that of a Na-poor and Ca-rich melilite. Abundant accessory minerals are mainly constituted by epidotes *s.s.*, Fe and Ti oxides, ilmenite, monazite, apatite, titanite and zircon. The abundant lithic fragments are represented by calcarenites that are sometimes metamorphosed, together with quartzites, siltstone, rocks of volcanic origin and glass. In sample THi 15, only calcarenite was observed. A few samples further show sporadic fragments of chamotte. Generally absent or very rare, the microfauna are represented by planktonic and benthic foraminifera.

Second layer The skeleton still greatly prevails over the matrix (Table 3), with the exception of sample THi 6; the latter being further characterized by high porosity and a smaller grain-size (about 180 μm) than the other samples (average 250 μm). The grain-size is particularly high (350–400 μm) in samples THi 19 and 20 (area XX). The average thickness of the layer is variable: it is rather thin in samples THi 1–4 (0.5–1.5 mm), intermediate in samples THi 6–11, 14

Table 3 *Second layer: the percentages of porosity, matrix and skeleton and the average grain-size obtained by image analysis. Samples are presented together when results showed a significant homogeneity*

Samples	*THi 1–4*	*THi 5*	*THi 6*	*THi 7*	*THi 8*	*THi 9, 13*	*THi 10*	*THi 11*	*THi 12*	*THi 14, 16–18*	*THi 19*	*THi 20*
Thickness (mm)	0.5–1.5	2.5–3.5	1.8–2.5	2.2–3.8	2.2–2.8	1.5–2.3	3.2–4.2	3.0–3.5	5.0–6.2	3.1–4.4	3.5–5.3	4.5–5.5
Porosity (%)	13	16	30	10	20	18	13	15	10	25	10	30
Matrix (%)	20	37	35	25	38	20	34	40	25	29	38	25
Skeleton (%)	67	48	35	65	42	62	53	45	65	46	52	45
Grain average dimensions (μm)	220	250	180	250	250	250	250	250	230	250	350	400

and 16–18 (1.8–4.4 mm), and thick in samples THi 12, 19 and 20 (3.5–6.2 mm). With respect to the first layer, the mineralogical assemblage does not change qualitatively, however, quartz is now far more predominant than the other phases.

Third layer Except for sample THi 12, the interface dividing the third from the second layer is generally evanescent. Both the thickness of the layers and the average grain-size are rather variable (Table 4). Microcrystalline calcite is the principal component. Quartz crystals of small dimensions are rare in samples THi 1–4 and 11, frequent in samples THi 6, 9, 10, 12–14 and 16–18, and abundant in the remaining samples. Fe and Ti oxides and epidotes *s.s.* are frequent in samples THi 6 and 11.

Sample THi 5 This sample shows at least three superimposed phases (Fig. 2), for a total of nine plaster layers and three white pigment layers. The three phases show the same sequence as previously observed. Excluding the thickness, the first and the second layers show the same characteristics in all the three phases. The matrix composition for the first phase is shown in Table 2. The third layer shows variable thickness (first phase, 350–550 μm; second phase, 150–300 μm; third phase, 350–600 μm) but comparable average grain-size (≥500 μm).

Pigments

Bright red, dark red, yellow, blue, green, black and white pigments have been identified by Raman micro-spectroscopy and SEM–EDS. The bright red pigment is made of cinnabar (Fig. 3 (a)). Crystals of appreciable dimensions form thick layers (average of 30 μm), over an undercoat of yellow ochre (Fig. 4 (a)). Since it was even mentioned by ancient authors (Pliny, *Historia naturalis*, 33, 118, 120; Vitruvius, *De architectura*, 7, 9, 5), the possible adulteration of the pigment has been checked. The addition of lead can be definitely rejected, while the introduction of Fe oxides is more controversial due to the presence of the yellow ochre undercoat.

The dark red pigment has been identified as red ochre (Fig. 3 (b)). Fine crystals of Fe oxides, phyllosilicates, calcite, quartz and rare feldspars were observed by SEM–EDS (Fig. 4 (b)). Raman micro-spectroscopy identified the Fe oxides as hematite. In samples THi 12 and 20, Fe oxides are more abundant and evenly distributed than in samples THi 1–3. In sample THi 20, the neat separation between the pigment and the support further suggests that the latter was already dried when it was decorated.

The yellow pigment is made of yellow ochre (Fig. 3 (c)). SEM–EDS and Raman micro-spectroscopy allowed the identification of goethite, quartz and phyllosilicates. The pigment layer

Table 4 *Third layer and pigment: 'Thickness' and 'Average grain-size have' been obtained by SEM–EDS; 'Pigment colour' has been described by the naked eye; 'Phase' has been determined by Raman micro-spectroscopy; 'Pigment name' refers to the Latin terminology. For sample THi 5, the measurements made on the third layer for the three phases are given in the text. Sample THi 15 has been omitted*

Thickness (μm)	*Average grain-size (μm)*	*Sample*	*Pigment colour*	*Pigment composition*	*Pigment name*
80–150	20	THi 1	Dark red + white	Red ochre + calcite	*Rubrica + creta*
		THi 2	Dark red	Red ochre	*Rubrica*
		THi 3	Dark red	Red ochre	*Rubrica*
20–50	20	THi 4	Dark yellow	Yellow ochre	*Sil*
280–650	≥250	THi 6	White	Calcite	*Creta*
400–600	≥280	THi 7	White	Calcite	*Creta*
500–800	≥500	THi 8	White	Calcite	*Creta*
20–70	≥250	THi 9	Green	Green earth	*Creta viridis*
120–240	≥50	THi 10	Dark red	Red ochre	*Rubrica*
400–550	≥220	THi 11	Dark green	Green earth + carbon black	*Creta viridis*
1000–1200	≥500	THi 12	Dark red + white	Red ochre + calcite	*Rubrica + creta*
20–70	≥250	THi 13	Green	Green earth	*Creta viridis*
500–850	≥380	THi 14	Bright red	Cinnabar	*Minium cinnabaris*
		THi 16	Bright red	Cinnabar	*Minium cinnabaris*
		THi 17	Bright red	Cinnabar	*Minium cinnabaris*
		THi 18	Dark blue	Egyptian blue + carbon black	*Atramentum*
320–500	≥400	THi 19	Light yellow + black	Yellow ochre + carbon black	*Atramentum + sil*
250–500	≥400	THi 20	Blue + dark red + dark yellow	Egyptian blue + red ochre + yellow ochre	*Caeruleum + rubrica + sil*

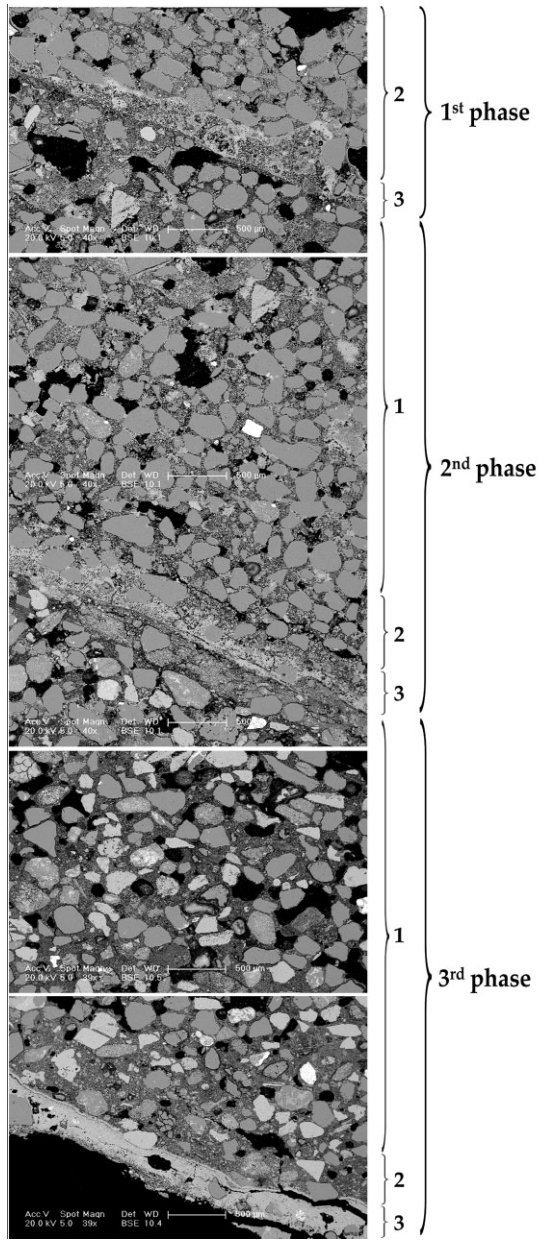

Figure 2 *SEM–BSE images representative of the three phases of sample THi 5.*

is thin in sample THi 4 (Fig. 4 (c)), but very thick in sample THi 20 (Fig. 4 (d)). The latter shows a few crystals immersed in a heterogeneous Ca-rich matrix. In Figure 4 (d), both the dark and the light grey portions are made of calcite, the dark portions being richer in Si and Al than the light aggregates. Quartz and phyllosilicates are always found in the darker matrix, while they are absent in the lighter aggregates. A likely hypothesis is that the darker matrix (similar to that of

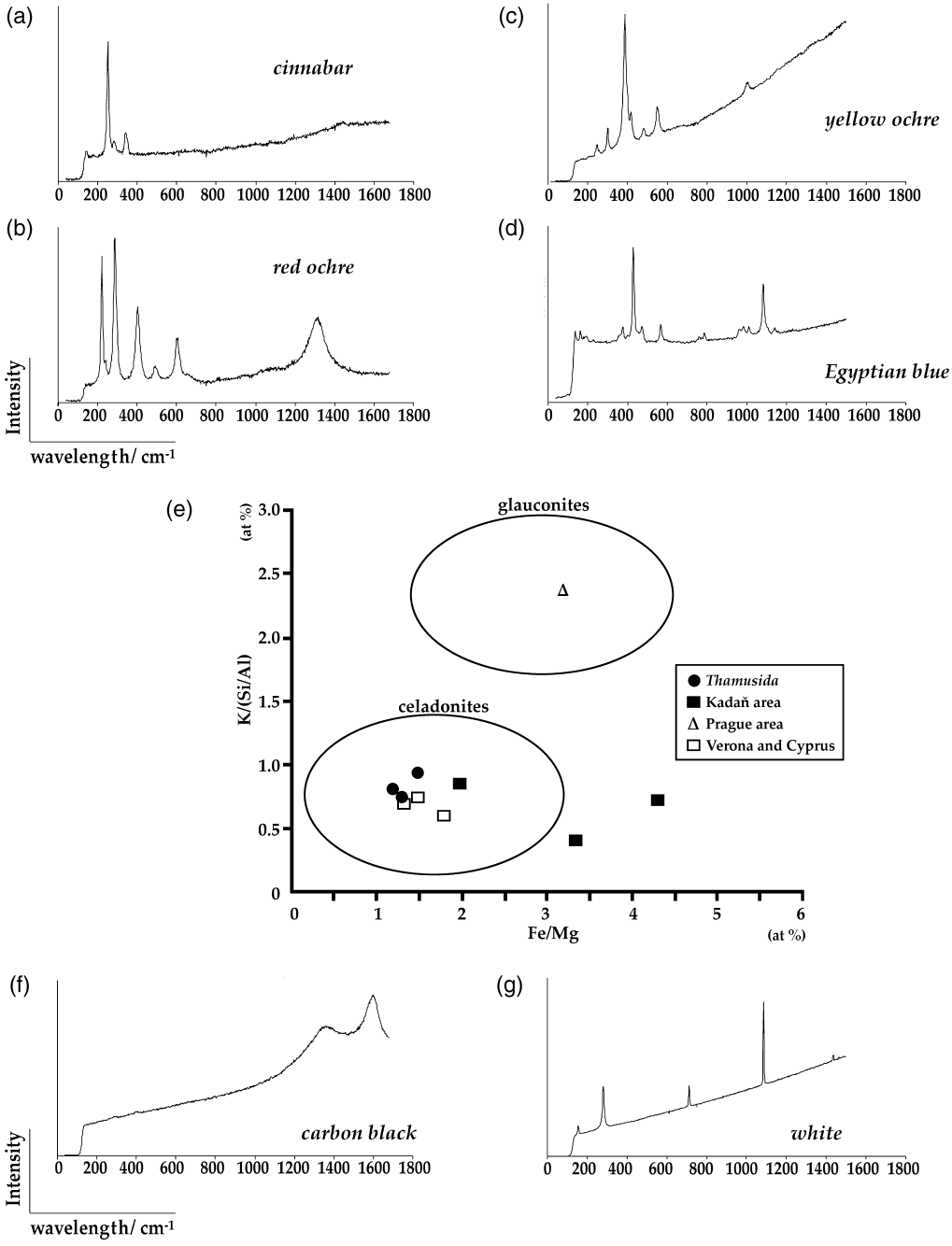

Figure 3 *Representative Raman spectra: (a) cinnabar; (b) red ochre; (c) yellow ochre; (d) Egyptian blue; (f) carbon black; (g) white. Intensities are expressed in arbitrary units. (e) SEM-EDS analyses on green earth; Fe/Mg–K/(Si/Al) binary diagram modified after Hradil* et al. *(2010).*

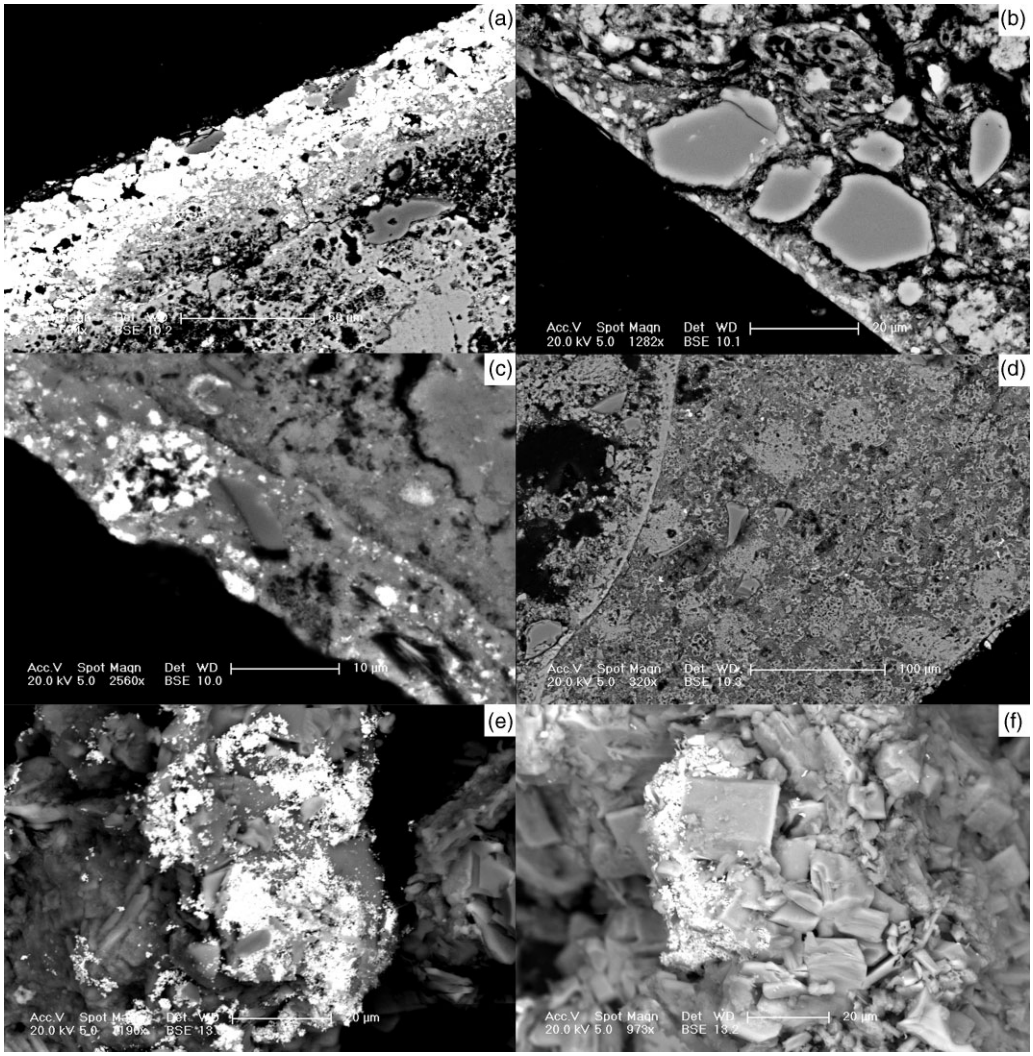

Figure 4 *SEM–BSE images of pigments in samples (a) THi 14, (b) THi 12, (c) THi 4 and (d) THi 20. Gold (e) and copper (f) nuggets in sample THi 22.*

sample THi 4) has been introduced with the yellow ochre pigment, while the lighter aggregates formed from lime mixed into the pigment.

Both the blue fresco pigments and the two blue beads are made of Egyptian blue (Fig. 3 (d)) of comparable composition (Table 5). SEM–EDS investigations further revealed the presence of rare tin, gold (Fig. 4 (e)) and copper (Fig. 4 (f)) nuggets, suggesting the reuse of scrap metals (see, e.g., Tite *et al*. 1984). In the blue beads, the transparent mineral is quartz, while the yellow encrustation consists of calcite.

The green pigment has been identified as green earth. Given the very similar structure and composition, the techniques used here can hardly distinguish celadonite ($(K_{0.8}Na_{0.01}Ca_{0.04})(Fe^{3+}_{1.31}Al_{0.28}Mg_{0.4})(Si_{3.58}Al_{0.42})_4O_{10}(OH)_2$; see Riederer *et al*. 1998) from

Table 5 *The SEM–EDS analyses. The green pigment shows crystals resembling a celadonite composition. Crystals analysed in the blue pigment applied to the plaster THi 20 and in the two blue spheres resemble cuprorivaite composition*

	Green pigment				*Blue pigment*			
	THi 13				*THi 18 n = 5*	*THi 20 n = 5*	*THi 21 n = 10*	*THi 22 n = 10*
	(wt%)	*(wt%)*	*(wt%)*		*(wt%)*	*(wt%)*	*(wt%)*	*(wt%)*
SiO_2	62.90	61.59	59.77	SiK	55.5	55.4	53.1	51.5
Al_2O_3	6.39	4.47	5.24	CaK	18.4	18.9	18.6	18.5
FeO	17.96	19.48	20.76	CuK	26.1	25.4	28.3	29.6
MgO	7.44	7.54	7.07	Total	100	100	100	100
K_2O	5.31	6.92	7.16					
Total	100	100	100					

glauconite ($K_{0.94}(Fe^{3+}_{0.72}Al_{0.42}Mg_{0.6}Fe^{2+}_{0.24})(Si_{3.9}Al_{0.1})_4O_{10}(OH)_2$; see Riederer *et al*. 1998). The phase in samples THi 9 and 13 seems comparable to that of celadonite, even if the K_2O and Al_2O_3 contents are, respectively, lower and higher with regard to the stoichiometric composition (Table 5). On the basis of Hradil *et al*. (2010), it is further possible to include our samples in the celadonite field from Cyprus and Verona (Fig. 3 (e)).

The Raman spectra of the black pigment showed two broad bands centred at about 1358 and 1600 cm^{-1}, allowing the identification of the carbon black pigment (Fig. 3 (f); Baraldi *et al*. 2006; Rampazzi *et al*. 2007). Given that carbon black was obtained from the carbonization of either wood or bone, the absence of calcium carbonate and/or phosphate (by SEM–EDS) suggests the vegetal origin of this pigment (Rampazzi *et al*. 2007, and references therein). Furthermore, the Raman spectra did not provide evidence of the band at about 960 cm^{-1}, which is indicative of the presence of $[(PO_4)^{3-}]$ (Dresselhaus *et al*. 1999). The vegetal origin of the pigment was definitely demonstrated by the colour change from black to whitish of a small fragment heated up to 450°C (Mazzocchin *et al*. 2010). Carbon black has been further used for darkening the green colour of sample THi 11 (green earth) and the blue colour of sample THi 18 (Egyptian blue).

Calcite—mostly microcrystalline—is the principal component of the white pigment used in samples THi 1 and 12 (Fig. 3 (g)). The layer thickness ranges from 20 to 250 µm and it is rarely exceeded by larger quartz crystals, which provoke irregularities along the outer surface.

DISCUSSION

Plasters

Raw materials Mineralogical and petrographical analyses allow direct correlation of plaster composition with that of both sands and clays locally available (Damiani and Gliozzo 2009; Gliozzo *et al*. 2011b). The plaster grain-size is comparable to that of local sands, but the mineralogical assemblage involves the utilization of clays as well. Quartz, feldspars, calcite and

micas are the principal constituents of sands, clays and plasters; pyroxenes, amphiboles and garnets are frequent in both clays and plasters, while absent or very rare in sands. These observations indicate diverse sources of raw materials and thus perhaps the use of a mixture of both sands and clays that outcrop nearby.

The abundance of lithic fragments may confer some relevant properties to these plasters, such as waterproofing. This technique is very different from that described by the ancient authors, but it can be compared to the addition of marble powders (Vitruvius, *De architectura*, 7, 3, 6) in numerous plasters of the Italic peninsula. In fact, neither the intentional addition nor the unwitting introduction of these lithic fragments can be conclusively verified. Lithic fragments are more abundant in plaster than in the natural raw materials; in this case, a deliberate addition seems likely. Conversely, a causal relationship seems to be lacking when correlating the abundance of lithic fragments to the use of the rooms (with or without the passage of water or vapours). As with other ancient production processes (Martinón-Torres and Rehren 2009), this evidence may trivially relate to local tradition and taste, without necessarily implying a deliberately developed technique.

The lime was probably produced using the local carbonate crust, which is the only Ca-rich sediment available in the vicinity of the site. The exploitation of this resource was suggested for mortar manufacture as well (Gliozzo *et al*. 2009a).

Plaster preparation and application *Thamusida* plasters generally showed three superimposed layers below the pigment. Equating the skeleton to the aggregate and the matrix to the binder, additional information on plaster recipes can be obtained. In theory, the aggregate:binder ratio should decrease from the first to the second layer, smoothing the bumps over in the first one. In practice, this happens for plasters of area VII and area XX, while those from the *thermae* show a variable trend. The extreme case is represented by samples THi 1–4, with a ratio of 1.3:1 in the first layer and 3.4:1 in the second. Excluding plasters from area XX, the average grain-size decreases reasonably from the first to the second layer in all the other buildings. As for the second layer, the absence of the coarse fraction (>250 μm) and the sharp decrease in lithic fragments indicates that the aggregate underwent sieving. The third layer is mainly made of calcite. The presence of quartz and feldspars should indicate the use of an impure carbonate material for lime production.

In general terms, the raw materials have mostly been used as received. Although the microscopic analyses made it possible to identify at least three plaster layers, they were very thin and rough. The overall manufacture was of low quality, and hence perfectly comparable to that observed in the Roman provinces (see, e.g., Aurigemma 1962; Barbet and Allag 1972; Abad Casal 1982; Davey and Ling 1982). More attention has been paid to the preparation and application of plasters in samples THi 14, 16, 17, 19 and 20, while all the others are of low quality (especially THi 15). Beginning from the middle–late Imperial age, a qualitative worsening of wall paintings has been observed in Roman provinces. Similarly at *Thamusida*, the plasters of the first century AD are qualitatively better than the later ones. The lack of spatic calcite (i.e., intentionally added) observed in the *Thamusida* plasters has also been noticed in some Roman provinces (Barbet 1995), such as Gaul (Barbet 1995; Barbet and Allag 1972), Britain (Davey and Ling 1982) and Tripolitania (Zliten villa; Aurigemma 1962). Similarly, in neighbouring Spain, the colours were applied on the last layer of sand and lime, while a layer of smooth white finish (up to a maximum of 2–3 mm) was rarely identified (Abad Casal 1982). Conversely, the addition of spatic calcite is mentioned by the ancient sources and well attested in Italy (Bianchetti *et al*. 1990).

Pigments

The pigments used were cinnabar, red ochre, yellow ochre, Egyptian blue, green earth, carbon black and calcite. Cinnabar was used exclusively in area VII, to decorate panels of bright red, alternating with narrow black or dark blue sectors (Cavari 2008). In the Roman provinces, cinnabar became rarer beginning from the middle of the first century AD (Barbet 1975; Davey and Ling 1982), when it was replaced by the red ochres (Barbet 1990). Analogously at *Thamusida*, cinnabar was applied in buildings of the first century AD only. The pigment was applied over a red ochre undercoat. This technical feature is attested in other provincial sites such as York (United Kingdom; Davey and Ling 1982), Dietikon (Switzerland; Béarat 1996) and Aix-en-Provence and Narbonne (France; Barbet 1998), and it is believed to be indicative of a late chronology (Barbet 1990). The purpose of this practice is not fully understood. Indeed, it would be plausible that the red ochre layer was applied in order to save the precious pigment (Barbet 1990). However, this intermediate layer could have been applied as a barrier, neutralizing the caustic lime (instead of wax, for example). In fact, cinnabar was known to be one of those pigments that alters if applied with a *fresco* technique.

Even taking into account the terminological confusion between red ochre, cinnabar and red lead, the ancient authors agreed that all cinnabar was coming from Spain, through the intermediation of Rome (Pliny *Historia naturalis*, 33, 118; Vitruvius, *De architectura*, 7, 9, 4; Cicero, *Orationes Philippicae*, 2, 48; Theophrastos' mention of 'Iberia' perhaps refers to another ancient country known by this name in Transcaucasian Georgia). However, the intermediation of Rome could have been illegally avoided. Commercial trading with southern Spain was well established (Gliozzo *et al*. 2009a) and it would not be the first time that the ancient authors have been contradicted. Conversely, there is no reason to doubt the credibility of the costs. Cinnabar was much more expensive than all the other colours, its price being established by law to a maximum of 70 *sesterces* per pound (Pliny, *Historia naturalis*, 33, 118). Therefore, the use of this pigment in area VII of *Thamusida* offers interesting insights into the prestige of the building, the workers engaged and the clients involved (Barbet 1990; Rozenberg 1996; Béarat 1997).

With the exception of area VII, the red pigments are made exclusively of red ochre. Yellow ochres were widely used at *Thamusida* as well. The wide availability of these two pigments at the top of the coastal calcarenites may have stimulated exploitation of the raw materials that were available nearby. Egyptian blue was used in areas VII and XX. The pigment used for plaster decoration shows a chemical composition comparable to that of the two blue beads found in area XXXVII; furthermore, in both cases scrap bronzes were used in place of malachite. Green earths were used for all green decorations.

CONCLUSIONS

Among the studies on the Roman world, this study provides new data on wall decorations at a provincial site. The comparison between present results and those available for other Mediterranean Roman sites frames *Thamusida* well within an aesthetic and technical *koinè* that differentiates sites of the peninsula from those in the Provinces. At *Thamusida*, the long-lasting use of the same raw materials (the sands and clays locally available) indicates a continuity in the supply of raw materials during the centuries of Roman occupation. Technically, a rather low level can be indicated for both the plaster preparation and the application. The surface finishes are also rough, with the exception of samples dated to the first century AD.

The identified pigments fall within the range of colours used in Roman times for fresco painting. Red ochre, yellow ochre, green earths, carbon black and calcite are widely used in all buildings, while cinnabar and Egyptian blue have been found in only two areas (VII and XX).

REFERENCES

Abad Casal, L., 1982, *La pintura romana en España*, Universidad de Alicante, Alicante.

Aurigemma, S., 1962, *Tripolitania—I monumenti d'arte decorativa II: Le pitture d'età romana*, Coll. L'Italia in Africa—Le scoperte archeologiche, Istituto Poligrafico dello Stato, Roma.

Baraldi, P., Bonazzi, A., Giordani, N., Paccagnella, F., and Zannini, P., 2006, Analytical characterization of Roman plasters of the '*Domus Farini*' in Modena, *Archaeometry*, **48**, 481–99.

Barbet, A., 1975, *Recueil général des peintures murales de la Gaule. I: Province de Narbonnaise, 1, Glanum* (Suppl. *Gallia* 27), Paris.

Barbet, A., 1990, L'emploi des couleurs dans la peinture murale romaine antique: 'marqueurs' chronologiques et révélateurs du 'standing' social? In *Pigments et colorants de l'Antiquité et du Moyen Âge. Teinture, peinture, enluminure, etudes historiques*, 255–71, Editions du Centre National de la Recherche Scientifique, Paris.

Barbet, A., 1995, La technique comme révélateur d'écoles, des modes, d'individualités de peintres? *Papers of the Netherlands Instute in Rome—Mededelingen van het Nederlands Instituut te Rome*, **54**, 61–80.

Barbet, A., 1998, La tecnica pittorica, in *Romana pictura. La cultura pittorica romana dalle origini al momento bizantino* (ed. A. Donati), 103–11, Electa, Milano.

Barbet, A., and Allag, C., 1972, Tecniques de préparation de parois dans la peinture romaine, *Mélanges de l'École française de Rome-Antiquité*, **84**, 935–1069.

Béarat, H., 1996, Chemical and mineralogical analyses of Gallo-Roman wall painting from Dietikon, Switzerland, *Archaeometry*, **38**, 81–95.

Béarat, H., 1997, Quelle est la gamme exacte des pigments romains? Confrontation des résultats d'analyse et des textes de Vitruve et de Pline, in *Proceedings of the International Workshop, Roman Wall Painting. Materials, Techniques, Analysis and Conservation, Fribourg, 7–9 March 1996* (eds. H. Béarat, M. Fuchs, M. Maggetti and D. Paunier), 11–34, Institute of Mineralogy and Petrography, Fribourg.

Bianchetti, P. L., Campisi, M., Gratziu, C., and Melucco Vaccaro, A., 1990, La calcite spatica dell'intonaco romano, in *Atti del VI Convegno di studi Scienza e Beni Culturali, Le superfici dell'architettura: le finiture, Bressanone, 26–29 Giugno 1990*, 251–60, Libreria Progetto, Padova.

Callu, J.-P., Morel, J.-P., Rebuffat, R., and Hallier, G., 1965, Thamusida. *Fouilles du Service des antiquités du Maroc*, École Française de Rome, Mélanges d'archéologie et d'histoire, Suppléments, no. 2, Editions de Boccard, Paris.

Carò, F., and Di Giulio, A., 2004, Reliability of textural analysis of ancient plasters and mortars through automated image analysis, *Materials Characterization*, **53**, 243–57.

Cavari, F., 2008, I rivestimenti parietali, in *Sidi Ali ben Ahmed*—Thamusida, *1. I contesti* (eds. A. Akerraz and E. Papi), 249–63, Quasar, Roma.

Cuomo di Caprio, N., and Vaughan, S. J., 1993, Differentiating grog (chamotte) from natural argillaceous inclusions in ceramic thin sections, *Archeomaterials*, **7**, 21–40.

Damiani, D., and Gliozzo, E., 2009, Le materie prime di *Thamusida*: i suoli argillosi, in *Sidi Ali ben Ahmed*—Thamusida, *2. L'archeometria* (eds. E. Gliozzo, I. Turbanti Memmi, A. Akerraz and E. Papi), 39–55, Quasar, Roma.

Damiani, D., Gliozzo, E., Turbanti, E. M., and Spangenberg, J. E., 2003, Pigments and plasters discovered in the house of Diana (Cosa, Grosetto, Italy), an integrated study between art history, archaeology and scientific analysis, *Archaeometry*, **45**, 341–54.

Davey, N., and Ling, R., 1982, *Wall-painting in Roman Britain*, Britannia Monograph Series, 3, Society for the Promotion of Roman Studies, London.

Delamare, F., 1983, Les peintures murales romaines de l'Acropole de Léro, *Revue d'Archéometrie*, **7**, 85–98.

Dresselhaus, M. S., Dresselhaus, G., Pimenta, M. A., and Eklund, P. C., 1999, Raman scattering in carbon materials, in *Analytical applications of Raman spectroscopy* (ed. M. J. Pelletier), 367–434, Blackwell Science, Oxford.

Duran, A., Jimenez De Haro, M. C., Perez-Rodriguez, J. L., Franquelo, M. L., Herrera, L. K., and Justo, A., 2010, Determination of pigments and binders in Pompeian wall paintings using synchrotron radiation – high-resolution X-ray powder diffraction and conventional spectroscopy – chromatography, *Archaeometry*, **52**, 286–307.

Edwards, H. G. M., Middleton, P. S., and Hargreaves, M. D., 2009, Romano-British wall painting: Raman spectroscopic analysis of fragments from two urban sites of early military colonisation, *Spectrochimica Acta Part A*, **73**(3), 553–60.

Gliozzo, E., 2007, Supplying Roman Italy with black and white pigments, in *Supplying Rome and the Empire* (ed. E. Papi), *Journal of Roman Archaeology*, Suppl. 69, 72–84.

Gliozzo, E., Dalconi, C., Cruciani, G., and Turbanti Memmi, I., 2009a, An approach to the investigations of mortars: the application of the Rietveld method, *European Journal of Mineralogy*, **21**, 457–65.

Gliozzo, E., Kockelmann, W. A., Bartoli, L., and Tykot, R. H., 2011a, Roman bronze artefacts from *Thamusida* (Morocco): chemical and phase analyses, *Nuclear Instruments and Methods in Physics Research B*, **269**, 277–83.

Gliozzo, E., Turbanti Memmi, I., Akerraz, A., and Papi, E. (eds.), 2009b, *Sidi Ali ben Ahmed*—Thamusida, *2. L'archeometria*, Quasar, Roma.

Gliozzo, E., Damiani, D., Camporeale, S., Memmi, I., and Papi, E., 2011b, Building materials from *Thamusida* (Rabat, Morocco): a diachronic local production from Roman to Islamic period, *Journal of Archaeological Science*, **38**, 1026–36.

Gliozzo, E., D'Aco, D., Memmi Turbanti, I., Galli, A., Martini, M., and Sibilia, E., 2009c, Common ware production at *Thamusida*: dating and characterisation of Roman and Islamic pottery, *Archaeological and Anthropological Sciences*, **1**, 77–85.

Gliozzo, E., Arletti, R., Cartechini, L., Imberti, S., Kockelmann, W. A., Memmi, I., Rinaldi, R., and Tykot, R. H., 2010, Non-invasive chemical and phase analysis of Roman bronze artefacts from *Thamusida* (Morocco), *Journal of Applied Radiation and Isotopes*, **68**, 2246–51.

Hallier, G., Marion, J., and Rebuffat, R., 1970, *Thamusida. Fouilles du Service des antiquité du Maroc*, 2, École Française de Rome, Roma.

Hradil, D., Píšková, A., Hradilová, J., Bezdička, P., Lehrberger, G., and Gerzer, S., 2011, Mineralogy of Bohemian green earth pigment and its microanalytical evidence in historical paintings, *Archaeometry*, **53**, 563–86.

Marion, J., and Rebuffat, R., 1977, *Thamusida. Fouilles du Service des antiquité du Maroc*, 3, École Française de Rome, Roma.

Martinón-Torres, M., and Rehren, Th., 2009, Post-medieval crucible production and distribution: a study of materials and materialities, *Archaeometry*, **51**, 49–74.

Mazzocchin, G. A., Vianello, A., Minghelli, S., and Rudello, D., 2010, Analysis of Roman wall paintings from the *thermae* of '*Iulia Concordia*', *Archaeometry*, **52**, 644–55.

Pagès-Camagna, S., and Colinart, S., 2003, The Egyptian green pigment: its manufacturing process and links to Egyptian blue, *Archaeometry*, **45**, 637–58.

Rampazzi, L., Campo, L., Cariati, F., Tanda, G., and Colombini, M. P., 2007, Prehistoric wall paintings: the case of the *domus de janas* necropolis (Sardinia, Italy), *Archaeometry*, **49**, 559–69.

Reinach, A., 1985, *Recueil Milliet: textes grecs et latins relatifs à l'histoire de la peinture ancienne*, C. Klincksieck, Paris.

Riederer, M., Cavazzini, G., D'yakonov, Y. S., Frank-Kamenetskii, V. A., Gottardi, G., Guggenheim, S., Koval', P. V., Müller, G., Neiva, A. M. R., Radoslovich, E. W., Robert, J.-L., Sassi, F. P., Takeda, H., Weiss, Z., and Wones, D. R., 1998, Nomenclature of the micas, *Canadian Mineralogist*, **36**, 905–12.

Rozenberg, S., 1996, Pigments and fresco fragments from Herod's Palace at Jericho, in *Proceedings of the International Workshop, Roman Wall Painting. Materials, Techniques, Analysis and Conservation, Fribourg, 7–9 March 1996* (eds. H. Béarat, M. Fuchs, M. Maggetti and D. Paunier), 63–74, Institute of Mineralogy and Petrography, Fribourg.

Tite, M. S., Bimson, M., and Cowell, M. R., 1984, Technological examination of Egyptian blue, in *Archaeological chemistry III* (ed. J. B. Lambert), 215–42, Advances in Chemistry Series, 205, American Chemical Society, Washington, DC.